# Journal of Materials Chemistry A

Accepted Manuscript


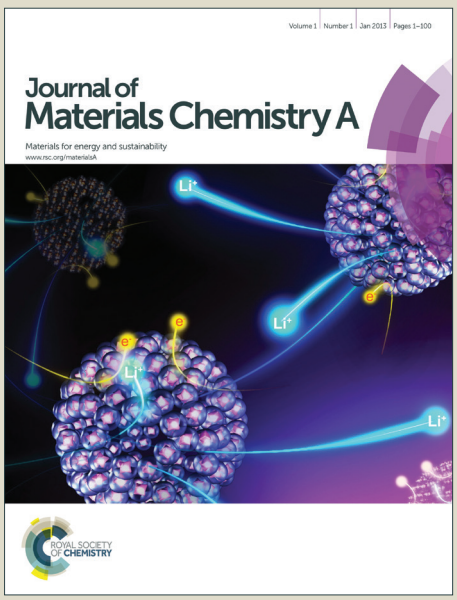





ROYAL SOCIETY OF CHEMISTRY

www.rsc.org/materialsA

Cite this: DOI: 10.1039/c0xx00000x

www.rsc.org/xxxxxx

ARTICLE TYPE

# Effect of graphene on the performance of an electrochemical flow capacitor†

**Soorya Sasi, Abhinav Murali, Shantikumar V. Nair, A. Sreekumaran Nair,* K. R. V. Subramanian,***

***Received (in XXX, XXX) XthXXXXXXXXX 20XX, Accepted Xth XXXXXXXXX 20XX***

**DOI: 10.1039/b000000x**

The Electrochemical Flow Capacitor (EFC) plays an important role in the energy storage field. The potential and ease of large scale energy storage of the EFC makes it highly adaptable in grid-scale energy storage. Current working models of the EFC operate with activated carbon and other coarse-sized carbon-based materials as input slurry materials, with limited device performance. Graphene is an excellent candidate for energy storage, having large specific surface area and also offers its advantages of being in the nano-carbon form. In this paper, we investigate the efficiency enhancement of an EFC device when graphene nanoplatelets-ionic electrolyte slurry was input into a flow device and charged/discharged, and compare it with the coarse and conventional graphite-aqueous electrolyte slurry. The performance evaluation of a newly developed composition of graphene-based slurry having high capacitance was carried out and this slurry was used for both static and dynamic energy storage devices. Thin film layers coated with this slurry have high electrode specific capacitance greater than 300 F/g, low-cost and nickel-free composition having relatively low toxicity. Intermittent flow device has shown a device capacitance of 64.5 F, 2 V with a 5 mL graphene slurry input, which corresponds to an energy density of 14.3 Wh/L. Device with graphite slurry has shown a capacitance of 2.3 F,1.6 V withan energy density of 0.422 Wh/L. When the graphene nanoplatelets-based slurry is used in the actual EFC full flow device, it gives 1.08 F, 2 V device performance with a slurry input of 24 mL. Additionally, the graphene nanoplatelets-based slurry when used together with the ionic electrolyte shows a better device EFC performance, *i.e* an energy density of 6 Wh/kg (0.064 Wh/L)) when compared to using a coarse graphite-based slurry (device capacitance of 0.75 F, 1.6 V, energy density of 2.2 Wh/kg (0.026 Wh/L)). Thus, this proof-of-concept study gives a significant difference in performance between a graphene slurry-based device and the conventional graphite slurry-based device. This model can be extended further by material modifications (such as addition of materials displaying Faradaic capacitance) to the slurry to realize better performing flow-based devices.

## Introduction

World's energy consumption has reached its peak[1] and this forces us to think proactively about renewable energy resources. While R&D in this area is going on, it is also crucial to store the produced energy efficiently. None of the storage devices presently available in the market is a perfect candidate to solve the problems in the energy storage field.[2] Batteries have established themselves and ruling the energy storage scenario[2,3] because of their higher energy density but they have no prowess where high power density is needed. Supercapacitors have penetrated to specific applications where high power density is needed. However, the energy that can be stored by a supercapacitor is only a fraction compared to that of a battery.[4] For large energy applications such as grid-scale energy storage, redox flow batteries and molten salt batteries could make new promises because of their great potential for scaling-up.[5] But they also have their own drawbacks such as slow charging and discharging, less life-span, etc. Here we emphasize the importance of flow capacitors[6,7] which can solve the disadvantages of batteries and supercapacitors and marry their advantages of high energy, high power, long life and ease of charge-discharge (rate performance), etc. Electrochemical flow capacitor (EFC) is a new concept of energy storage mechanism which hasthe advantages of both batteries and supercapacitors. EFC is a flow capacitor that has adopted the electrolyte flowing mechanism of flow batteries and charge storage principle of EDLCs (electric double-layer capacitors). In an EFC, the electrode material stores the ions from the electrolyte, hence stores charge like static EDLCs but electrode material is in a flowable manner. The working of EFC has been explained in recentliteratures.[6,7] Carbon-based slurry (carbon + electrolyte) is filled in containers outside the flow cell. On charging, it is pumped into the flow cell and charge is stored in the carbon particles electrostatically as shown in **Fig.1**. Previous studies[6,7] reported the use of various carbon materials like phenolic resin-derived activated carbon beads, non-spherical carbide-derived

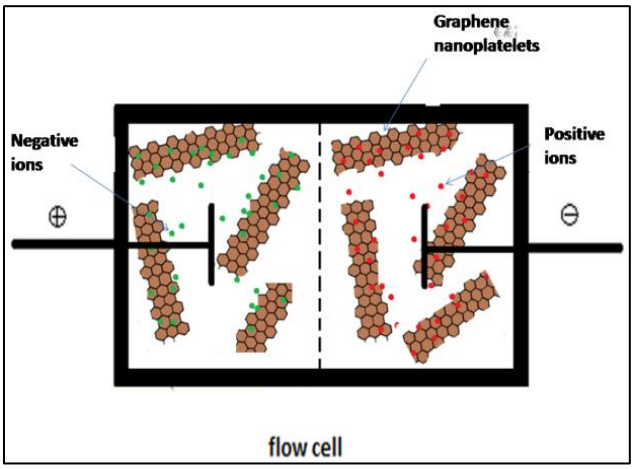


**Fig.1.**A schematic of the charge storage mechanism in a flow cell.The image depicts the electrostatic interaction of ions with graphene.

carbon powder, carbon black-added activated carbon, etc., which were all in micron-size range. Drastic improvement in electrical properties as well as storage capacity of a carbon material when its size comes to a nanoregime is a proven concept.[8] Specific surface area increases as the size decreases and high specific surface area is a desirable characteristic of an electrode material of any energy storage device. Carbon nanotube, graphene, fullerene etc. are the well-known nanocarbon forms which have manifested their efficiency as electrode materials in devices.[8,9] Here we investigatedtheelectrochemical flow capacitor performance of graphene nanoplatelets-based slurry and comparedthe same with micron-sized ball-milled graphite-based slurry (as control). The graphene-based slurry gave a better performance in both intermittent- and full-flow devices. Graphene-basedslurry in intermittent flow capacitor gave a capacitance of 64.5 F with 2V which corresponds to an energy density of 14.3 Wh/L (179 Wh/Kg) with a total slurry input of 5mL. When the graphene-based slurry was used in the actual EFC full-flow device, it gave a 1.08 F, 2 V device with a total slurry input of 24 mL. Additionally, the graphene nanoplatelets-based slurry when used together with the ionic electrolyte showed a better device EFC performance with energy density of 6 Wh/kg (0.064 Wh/L) when compared to using a coarse graphite-based slurry (device capacitance of 0.75 F, 1.6 V, energy density of 2.2 Wh/kg (0.026 Wh/L). Thus, this proof-of-concept study gave a significant difference in the performance between a graphene slurry-based device and a conventional graphite slurry-based device.

Performance of EFC can be improved by expanding the contact area of current collectors exposed to the flowing slurry. For that purpose, modifications in the present design of current collectors have been probed. This study also reports the performance improvement of static EDLC electrodes coated with the graphene slurry (specific capacitance upto 300 F/g) by different coating methods, when compared to static EDLC electrodes coated with graphite-based slurry. To prepare such electrodes, we introduced an in-house coating method in which the wastage of slurry was minimum while producing good graphene coatings.The study can be further extended in future by modifying the electrochemical nature of the slurry by including materials showing good Faradaic capacitance behaviour such as $RuO_2$ nanoparticles, etc.

## Experimental Section

### 1. Study on static EDLC supercapacitor electrodes and cells

Two samples *i.e*, commercial graphene and in-house graphene were used for a comparison study, where graphite was the control. Commercial graphene nanoplatelets were bought from Reinste Nanoventures, New Delhi, India. In-house graphene was prepared by the following wet ball-milling method reported earlier.[10] About 700 mg of graphite fine powder was mixed with 35 mL of methanol and 3 mL of distilled water. About 11.5 mg of 1-pyrene carboxylic acid (exfoliating agent) was added to this mixture. The whole mixture was ultrasonicated for 30min and ball-milled (Retsch, PM 400, Germany) for 60 h with 300 rpm and 30 min resting time after each 30 min running. Two jars with four stainless steel balls in each jar were used for the milling. The resultant slurry was dried and graphene powder was obtained.

Both commercial and in-house graphene were characterized using Raman spectroscopy (Confocal Raman Spectrometer (WITEC ALPHA 300 RA with a laser of 486 nm and a spot size > 2 µm). Atomic Force Microscopy (AFM) was done with a JEOL SPM 5200 machine. Wide angle powder X-ray diffractionwas done with CuK$\alpha$ (1.54 Å) radiation using an X'Pert PRO Analytical instrument. An electrode coated with graphite-based slurry was used as the control. Graphite fine powder of 2 µm size was obtained by dry ball-milling (with 300 rpm for 30 h with a resting period of 30 min after each 30 min milling). In each jar, 700 mg of graphite powder mixed with 11.5 mg sodium lauryl sulphate and four stainless steel balls were used. All the samples were analysed by using a four-probe (JANDEL MODEL RM 3000 (using a probe current of 99 mA) conductivity test where the probe distance was 40 µm. For four-probe testing, samples were pelletized using a pelletizerto 1 cm circular sheets and the sheet resistance was directly measured by using the four-probe. Conductivity values of the sheets were calculated from the sheet resistance. Surface areas of commercial- and in-house graphenes and graphite were analysed by using $N_2$adsoption-desorptionBET(Brunauer-Emmett-Teller) analysis (Micromeritics,TriStar 3000 V6.07 A- 2050).

The graphene slurry for electrode coatings was prepared as follows: about 10 mg of graphene was mixed with 150 µL of isopropyl alcohol (Nice chemicals, India), 0.1 mg sodium lauryl sulphate ((SLS),Nice chemicals, India)) and 25 µL of oleyl amine (Sigma Aldrich, US). This slurry was coated on titanium plates by doctor-blading and in-house spray coating methods, respectively. Excess amount of SLS on the coatings was washed-off with 2-ethoxy ethanol (Nice chemicals, India) and distilled water, respectively. Graphite slurry, for the control, was prepared by the same method and composition with graphite instead of the graphene.

The in-house spray coating method gave better, uniform coatings with less amount of slurry than the doctor-blading, where the spray coating equipment was made up of a syringe with a spraying nozzle on its mouth as shown inthe **electronic supplementary information**, **ESI (1A)**. The coated samples were as shown in **ESI (1B).** The thickness of the films obtained

with the help of a profilometer(Veeco,Dektak 150,VDS440QS, USA) is shown in **ESI (1C)**.

The electrochemical characteristics of the graphite and the graphene electrodes were analyzed using cyclic voltammetry,[11] charge-discharge and electrochemical impedance spectroscopy, respectively. A three-electrode study gave electrode performance, while a two-electrode study gave cell/device performance. For the three-electrode study, graphite and graphene electrodes were tested with various aqueous electrolytes (1M) such as potassium hydroxide (KOH), sodium hydroxide (NaOH), lithium hydroxide-lithium nitrate mixture (50% LiOH+50% $LiNO_3$), lithium hydroxide (LiOH), lithium nitrate ($LiNO_3$), respectively, and the commercial graphene electrodes with an ionic electrolyte 1-butyl 1-methyl pyrrolidiniumbis(trifluoromethylsulfonyl)imide (with a potential window of 3.5 V for two-electrode study) as in **ESI (2)**. Cyclic voltammetryof graphite electrodes was carried out at 10 mV/s scan rate and a voltage window of 1V, 1V, 0.45V, 0.65V and 1.4V for the above mentioned aqueous electrolytes, respectively, as in **ESI (3**) and charge-discharge study for 5 mA charging and discharging current densities. The specific capacitance of electrodes and cells/devices was calculated by using the equations (1) and (2), respectively.

For 3 electrode CV testing,

$$Csp = \int idv/\Delta v\ (dv/dt).m \quad (1)$$

For 2 electrode CV testing,

$$Csp = 2\int idv/\Delta v\ (dv/dt)(m1 + m2) \quad (2)$$

Where *C*sp is the specific capacitance, $i$ is the current, $\Delta v$ the voltage window and $m$ is the weight of the active material (m1 and m2 are the weights of the active materials of the two electrodes). A factor of 2 was applied for the specific capacitance calculations for the two-electrode study because the two-electrode system resembles the two capacitors connected in series. Specific capacitance was calculated from the slope of the discharge curve of charge-discharge study by using the equation (3) for three-electrode study and equation (4) for two-electrode study.

$$Csp = i/m \times \frac{dv}{dt} \quad (3)$$

$$Csp = 2i/(m1 + m2) \times \frac{dv}{dt} \quad (4)$$

**2. Study on electrochemical flow capacitor**

**Fig. 2A** shows the schematic diagram of the electrochemical flow capacitor. Electrochemical flow capacitor was assembled as shown in **Fig. 2B** with a modification in current collector design, for more area of contact between flowing slurry and current collectors. Inside each sub-compartment, there were two current collector plates inter-connected as shown in **Fig. 2C**. The current collectors were made up of stainless steel. All containers and the flow cell were made up of an insulating material. PTFE (poly tetrafluoroethylene) was used as the separator. Peristaltic pumps were used for pumping and withdrawing the slurry. Pump's speed (rpm) vs. flow rate is given in **ESI (4).** A proper flow rate was determined from **ESI (4**), such that the storage containers mentioned in **Fig. 2A** and **B** were filled to an optimum level (without overflow) and the slurry was fed into the main chamber with the help of peristaltic pumps without leakages through the connecting pipelines. They were different in intermittent-flow and full-flow devices as in intermittent flow, only incremental volumes were to be fed inside the main chamber as opposed to full flow where the complete slurry volume was fed in one-shot.

Graphite slurry (control) to be loaded in EFC was prepared in the following manner. To get 100 mL slurry, 1.2 g of ball-milled graphite fine powder was mixed with 36 mL of isopropyl alcohol, 3 mL of oleyl amine, 12 mg of sodium lauryl sulphate and 40 mL of 1 M LiOH. The graphene-based slurry was prepared using commercial graphene nanoplatelets, oleylamine, sodium lauryl sulphate, isopropanol and ionic electrolyte 1-butyl 1methyl pyrrolidiniumbis(trifluoromethylsulfonyl)imide, while the electrolyte was 50% v/v ionic electrolyte mixed with 50% v/v propylene carbonate with added additive viz., 5 M camphor sulphonic acid. The volume ratio of the ionic electrolyte in the entire slurry was 40% while the remaining constituents made-up the 60%. 100 mL slurries were prepared and the typical amounts of the various constituents in the slurry were as follows: 20 mL 1-butyl 1-methyl pyrrolidiniumbis(trifluoromethylsulfonyl)imide, 20 mL propylene carbonate, 2 mL of 5 M camphor sulphonic acid, 1.2 g graphene nanoplatelets, 3 mL oleylamine, 12 mg of sodium lauryl sulphate and 36 mL isopropanol. For the in-house graphene slurry, the commercial graphene platelets were replaced by the in-house graphene. Oleylamine in the slurry helps to modify the graphene sheet edges and dangling bonds to provide limited functionalization.

Sodium lauryl sulphate is a surfactant which helps to anchor the graphene onto the current collectors. Isopropyl alchohol provides a less viscous, slowly evaporating medium for adjusting the rheological nature of the slurry.

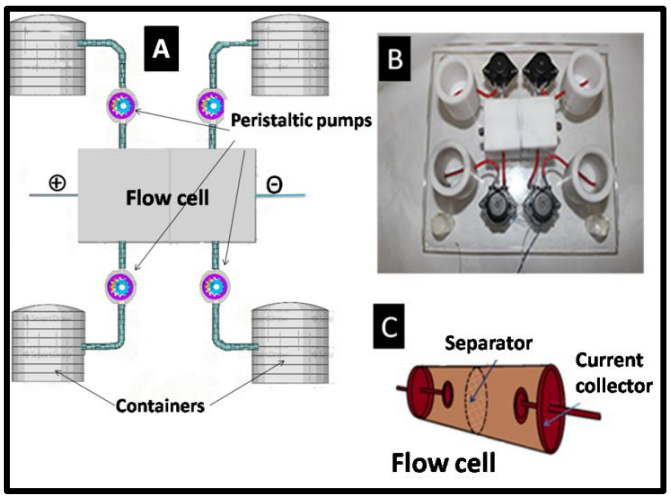


**Fig.2**. A –a schematic diagram of EFC, B –a lab-scale EFC device setup, C- modification of current collectors.

The EFC device performance was analyzed by using chronoamperometry[12] with both in-house graphene and the commercial graphene slurries, while the graphite slurry was the control. Flow device capacitance in Farads (F) and device specific capacitance in F/g was calculated from the chronoamperometry charging curve by the equations (5a and 5b) and energy density (from the chronoamperometry charging curve) and power density (from the chronoamperometry discharging curve) were calculated by using the equations (6a & b) and equation (7), respectively. Cycling study of the EFC was done for 130 cycles in LiOH electrolyte with an applied voltage of 1.5 V for 500 s charging time and discharging time each.

$$C = 2/\Delta E \ . \int i dt \quad (5a)$$

Where $C$ is the device capacitance, $\Delta E$ the potential applied, $i$ is the current and $m$ is weight of active material.

$$Csp = 2/\Delta E m \ . \int i dt \quad (5b)$$

Where Csp is the specific capacitance.

$$\text{Energy density} = \int i dt . v/3600 . m \quad (6a)$$

Symbols are already mentioned in previous equations.

$$\text{Volumetric energy density} = \int i dt . v/3600 . \text{vol} \quad (6b)$$

$$\text{Power density} = \frac{i1.V + i2.V + i3.V + i4.V + i5.V + i6.V + i7.V + i8.V + i9.V + i10.V}{10} . m \quad (7)$$

Where $i1$, $i2$, etc. are random current values from the $i$-$t$ discharge graph.

The volumetric power density=

$$\frac{i1.V + i2.V + i3.V + i4.V + i5.V + i6.V + i7.V + i8.V + i9.V + i10.V}{10} . \text{vol} \quad (8)$$

## Results and Discussions

Graphene powder obtained (both in-house and commercial) was analyzed with Raman spectroscopy, XRD and AFM, respectively. Raman spectrum was taken to establish the signature of graphene and estimate the number of layers and defect density from the peak intensities. The Stokes photon energy shift caused by 532 nm laser excitation of single-layered graphene results in 2 peaks in the Raman spectrum: an in-plane vibrational mode (G band) at 1580 $cm^{-1}$, a second order overtone of a different in-plane vibration (D band) at 1350 $cm^{-1}$ and a 2D peak at 2690 $cm^{-1}$. It is well-known that as the number of graphene layers increases, the spectrum of graphene changes; basically the 2D peak will split into several modes which combine together resulting in a broader, shorter and higher frequency peak. The G peak will also undergo a similar red-shift with increase in the number of layers of graphene. A comparison of the Raman spectrum of in-house and commercial graphene with that of graphite is shown in **Fig. (3)**. The spectra have been vertically offset for clarity. The D band position of commercial graphene, in-house graphene and graphite was located at 1359, 1368 and 1380 $cm^{-1}$, respectively, while the

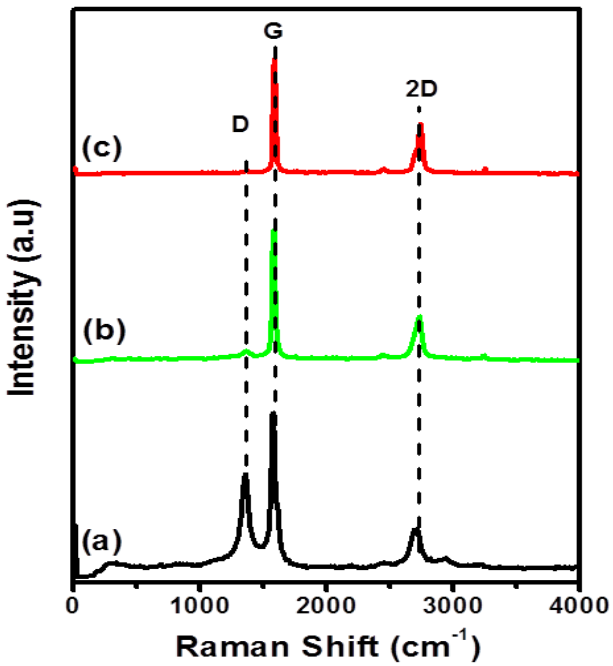


**Fig. 3.** Raman spectra of commercial graphene, in-house graphene and graphite, (a) commercial graphene, (b) in-house graphene and (c) graphite.

G band of commercial graphene, in-house graphene and graphite was located at 1570, 1581 and 1593 $cm^{-1}$, respectively. The 2D band of commercial graphene, in-house graphene and graphite was at 2702, 2738 and 2750 $cm^{-1}$, respectively. The trends in Raman spectra are indicative of the presence of a few-layer graphene in the materials used. The commercial graphene showed more down-shift in the 2D band position than in the in-house graphene indicating that it has lesser number of layers. The $I_{2D}/I_G$ ratio of commercial and in-house graphene was 0.933 and 0.67, respectively. The $I_D/I_G$ ratios of commercial graphene, in-house graphene and graphite were 0.963, 0.531 and 0.679, respectively. This is indicative of the fact that the commercial graphene possess more defects than in the in-house graphene.

**Fig. 4 and 5** show the TEM images of the in-house graphene and commercial graphene in different magnifications. The images clearly indicate that both in-house and commercial graphene

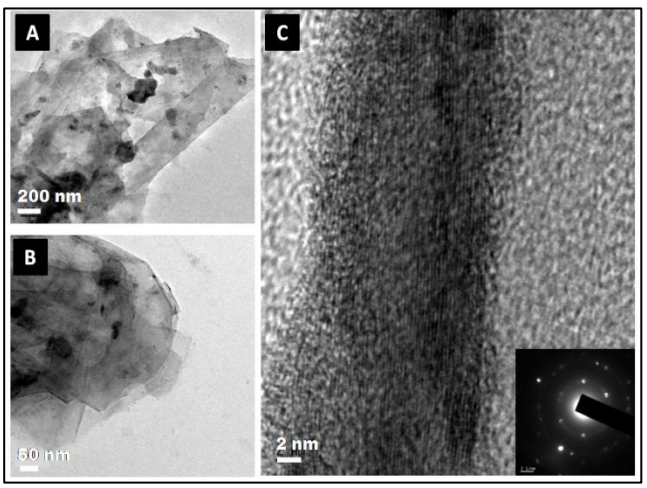


**Fig. 4**. TEM images of the in-house graphene.

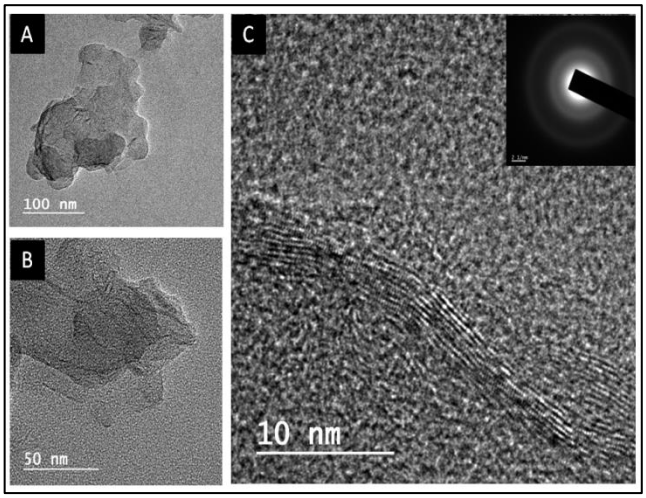


**Fig. 5**. TEM images of commercial graphene.

consist of a few layered graphene sheets. Inset of **Fig. 4c** shows a SAED pattern showing both diffused rings and dots indicating the random overlay of individual platelets. This is in agreement with the HRTEM results. Similarly, commercial graphene also revealed partially ordered crystal structure as evident from HRTEM image and the SAED pattern (**Fig 5c**). Commercial graphene had more amorphous nature, which can be attributed to the presence of more defects in comparison to in-house graphene.

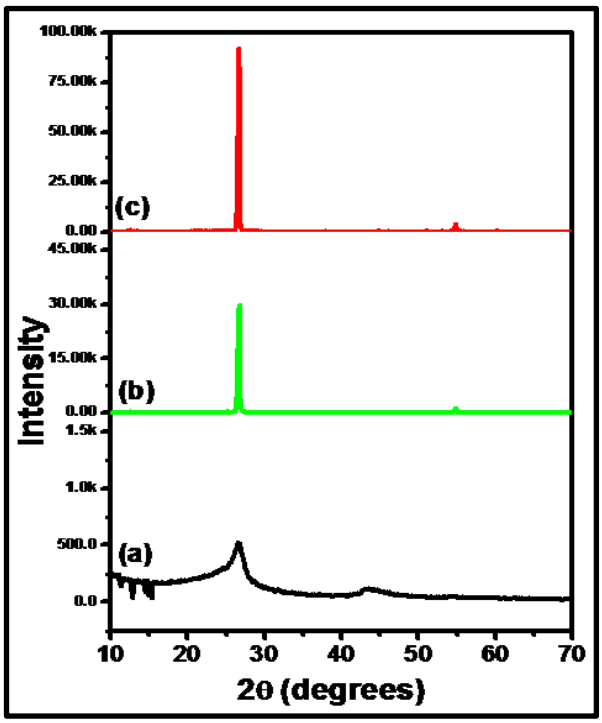


**Fig. 6**. XRD pattern of a) commercial graphene, b) in-house graphene and c) graphite, respectively.

XRD was also done to evaluate the degree of crystallinity of the carbonaceous layers. A comparison of the XRD patterns of in-house and commercial graphenes with graphite is shown in **Fig. 6**. Raw graphite showed a very strong peak at $2\theta = 26.60°$ corresponding to diffraction from the (002) plane (trace c in **Fig. 6**). In-house graphene showed a relatively weaker (002) plane diffraction possibly suggesting a reduction in the number of graphene layers. Commercial graphene displayed a very weak and broad peak at 26.60°.

The commercial and in-house graphenes were further characterized by AFM. A typical AFM topography of the commercial and in-house graphenes is shown in **Fig. 7**. From the height profiles (shown as inset in **Fig. 7 A & B**), the number of layers was estimated to be 9 and 17, respectively for commercial and in-house graphene samples. The lateral dimensions of commercial graphene was found to be much smaller than those in the in-house graphene. The conductivity of the carbon materials was analyzed by four-probe measurments. From four-probe testings, the conductivity of the commercial graphene, in-house graphene and graphite were found to be $7.5\times10^4$ S/m, $3.1\times10^4$ S/m and $1.2\times10^4$ S/m, respectively. The surface areas of the carbon materials from BET measurements were found to be 720 $m^2/g$, 212 $m^2/g$ and 6 $m^2/g$, respectively, for commercial and in-house graphenes and the graphite.

Commercial and in-house graphenes and graphite electrodes were tested using cyclic voltammetry and galvanostatic charge-discharge measurements. Graphite electrodes were tested with various electrolytes (1 M) such as $LiNO_3$, LiOH, NaOH, KOH, anda 50:50 mixture of LiOH and $LiNO_3$, respectively. The electrode in LiOH gave a specific capacitance value of 70 F/g under a three-electrode CV study and 10 F/g in a two-electrode CV study with a scan rate of 10 mV/s and potential window of 0.65 V and 0.7 V, respectively. The graphs are shown in **ESI (5)**. On the other hand, the graphene samples gave good specific capacitance values when analyzed using the three-electrode as well as two-electrode CV studies. Spray-coated samples gave higher values as compared to the doctor-bladed and EPD (electrophoretically deposited) samples. The commercial graphene sample gave an average specific capacitance value of 300 F/g and 120 F/g with a scan rate of 10 mV/s for the three-electrode and two-electrode CV studies, respectively, with the LiOH electrolyte and a voltage window of 0.48 V for three-electrode study and 1.6 V for two-electrode study (**ESI (6)).** In the ionic electrolyte, 1-butyl 1methyl pyrrolidiniumbis(trifluoromethylsulfonyl)imide), the specific capacitance values were 250 F/g for the three-electrode CV study and 72 F/g for the two-electrode study with a potential window of 4.5 V. In-house graphene gave specific capacitance values of 80 F/g at a potential window of 0.55 V and 35 F/g at a potential window of 1.6 V in LiOH for three- and two-electrode studies, respectively, (**ESI (7**)) and a capacitance of 40 F for the two-electrode study in ionic electrolyte with a potential window of 3 V (**ESI (8**)).

Galvanostatic charge-discharge study of graphite showed almost same values of specific capacitance (68 F/g and 10 F/g) for three- and two-electrode studies, respectively, similar to the values obtained from the CV studies. Both commercial and in-house graphene gave almost same specific capacitance values (**commercial** -120 F for aqueous electrolyte and 70 F for ionic electrolyte, **in-house** – 31 F for aqueous electrolyte and 40 F for ionic electrolyte, respectively) as that of the same from the two-electrode study. Graphene samples were analyzed using electrochemical impedance spectroscopy as well, **ESI (9**).

Cite this: DOI: 10.1039/c0xx00000x

www.rsc.org/xxxxxx

ARTICLE TYPE

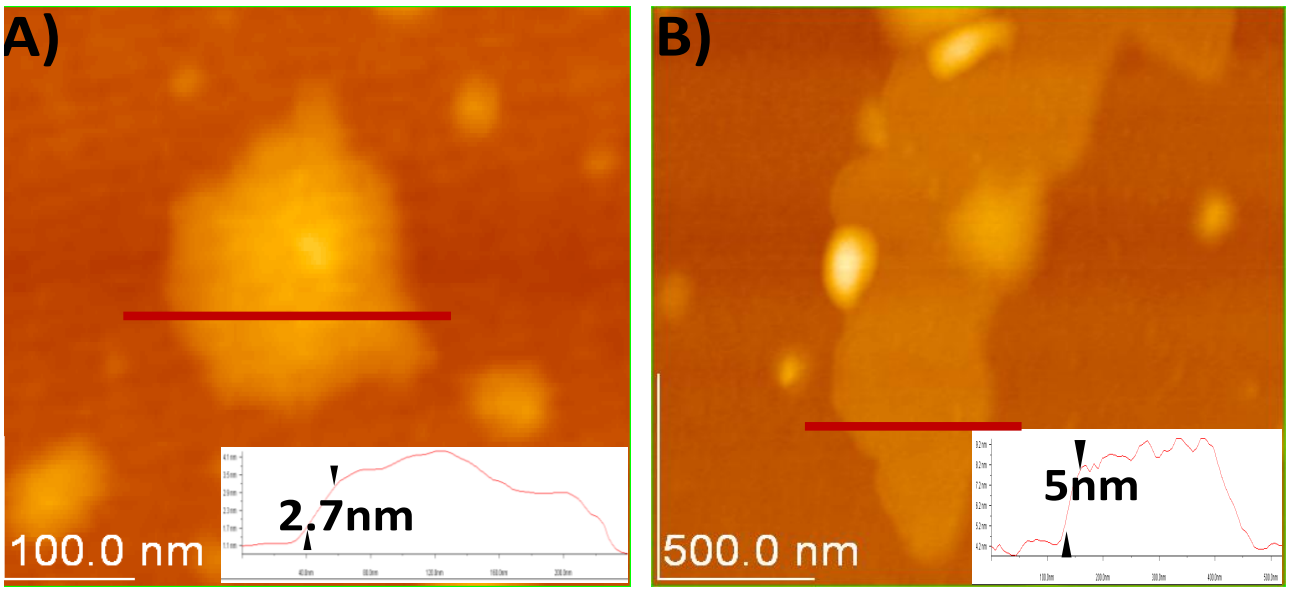


**Fig. 7.** AFM images of A) commercial graphene. The number of layers was estimated to be ~ 9, B) in-house graphene which has ~17 layers.

The use of graphene in the slurry for the EFC resulted in an enhancement in the storage capacitance because of the following reasons: a) graphene nanoplatelets have a high specific surface area, and b) the formation of 3-D pore networks due to the linking of the graphene nanoplatelets by the amine and the surfactant (SLS) leading to good ion interactions in the EDLC. This combination of slurry has a very good adhesion on metal plates like titanium, nickel and aluminium as compared to the EPD coatings, which is a favourable characteristic for the long-lasting charge storage and life-span of such devices. Spray-coated samples have smoother thin coatings and the spraying helped the graphene nanoplatelets to create very good 3D-networks without any compression unlike that encountered in doctor-blading. This can be judged as a stepping stone to the flow-based system where the graphene platelets are freer and not compressed and stacked by using mechanical forces (as in doctor-blading), which helped to create a porous surface that can interact with electrolyte more effectively.

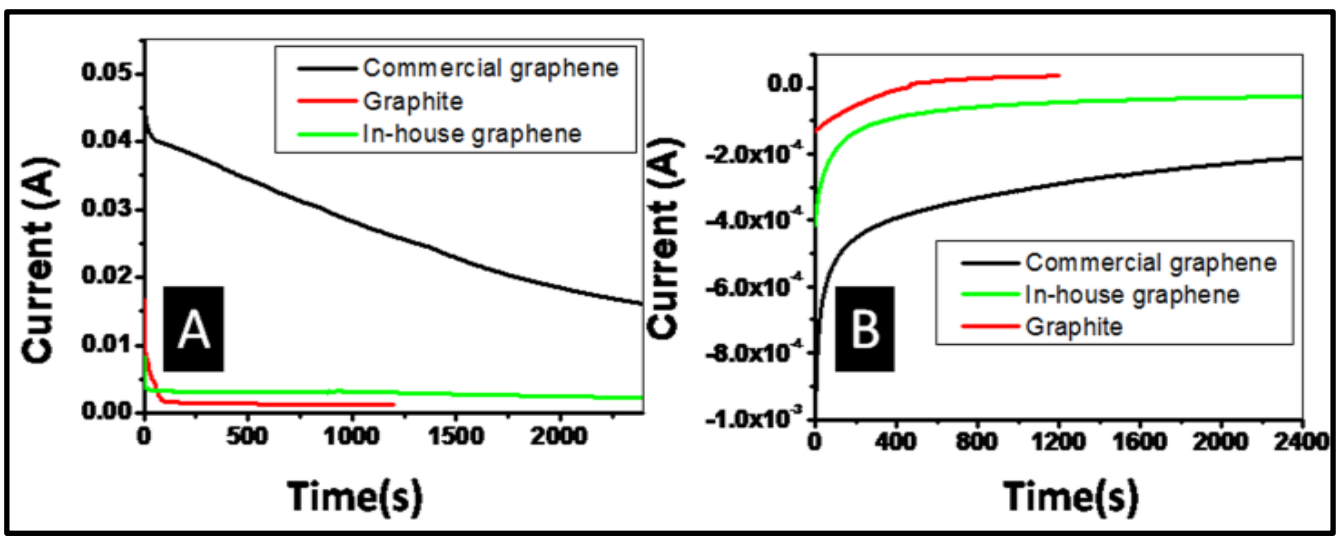


**Fig. 8.** Intermittent EFC performance: (A gives charging behaviour and B gives discharging behaviour)

To elaborate and discuss the working of EFC *i.e*, on charging, the positive ions from the electrolyte get attracted towards the negatively-charged graphene nanoplatelets and negative ions from the electrolyte get attached to the positively-charged graphene nanoplatelets. The sheet-like morphology and the higher surface area of the 3-D networked graphene platelets anchor more ions and hence more amount of energy has been stored. The structure modification of the current collectors gave more probability of charge induction to the graphene nanoplatelets. While discharging, graphene nanoplatelets can dispense all the charges back easily and quickly on account of the open-pore structure. This improves the power of the device. Intermittent EFC device performance is shown in **Fig. (8**). The commercial graphene showed higher performance when compared to graphite. The commercial graphene slurry-based device of 64.5 F and 2 V gave an energy density of 14.3 Wh/L and power density of 0.3 W/L, respectively. In-house graphene-based device yielded 6.8 F and 2 V with an energy density of 1.5 Wh/L and power density of 0.08 W/L and the graphite-based device yielded 2.3 F and 1.6 V with an energy density of 0.47 Wh/L and power density of 0.013 W/L.

In addition to CV studies, chrono-amperometry was also used to measure the charging and discharging response. EFC, being a flow device, the contributions to the distortion of the charging and discharging curves are expected to be minimal as the flow conditions even out the electrical field and hence the resistance elements and capacitance elements are transient. Charging and discharging graphs are shown in **Fig. (9**). In the present case, the charging curve is used to compute the device and specific capacitance as well as the energy density. Power density is computed from the discharging curve. However, it is observed that capacitance computed as C=Q/V from the charging curve is higher than that computed from the EFC discharging curve. We have considered the higher value of 2F as representing the true device capacitance which realizes the complete flow of charges into the system and its effective storage in the dynamic EDLC layers. The discharge curve is probably highly distorted due to contribution from resistance elements in the flow. Thus the coulombic efficiency needs further improvement, which will be the basis of future studies. Cycling study of the device was carried out for 130 cycles with 1.5 V applied voltage and 500 s each charging and discharging time by using chronoamperometry. A steady performance was obtained without much decay as shown in **Fig. (10).** For full-flow EFC device testing, charging was done at constant voltage of 2 V for 2400 s. The calculated device capacitance for commercial graphene was 1.082 F. The calculated energy density was 0.064 Wh/L (6 Wh/kg considering only the active graphene mass), for a total slurry volume of 24 mL. Discharging was done at 0 V for 2400 s. The average power density was 0.013 W/L. For the graphite slurry, charging was done at constant voltage of 1 V for 1200 s. The calculated device capacitance was 0.75 F. The calculated energy density was 0.02 Wh/L (2.2 Wh/kg considering only the active graphite mass) for a total slurry volume of 24 mL, then the discharging was done at 0 V for 1200 s. Average power density was 0.004 W/L. These results further confirm the enhancement in performance of the device when graphene slurry was used for the EFC. We can state that the nanosize of graphene helped in the improvement of energy storage and hence the capacitance. The ionic liquid has played a vital role in improving the voltage window.

The novel mixture of graphene, oleylamine, isopropyl alcohol and sodium lauryl sulphate gave good rheological properties and a fine mixture which was not clogging and acted as an excellent coating material for both the static and dynamic devices with a good capacitance value. Oleylamine in the slurry helps to modify the graphene sheet edges and dangling bonds to provide limited functionalization. Sodium lauryl sulphate is a surfactant and helps to anchor the graphene onto the current collectors. Isopropyl alchohol provides a less viscous, slowly evaporating medium for adjusting the rheological nature of the slurry. The amine addition can provide marginal improvements in conductivity**.** Graphene platelets produced a honey comb-like structure with good conductivity, high electron mobility as well as good surface area and hence more energy storage ability. Graphene has an ability to increase energy density, that is the amount of energy stored in a given volume. This implies that efficient storage devices which are smaller and durable are possible without compromising the

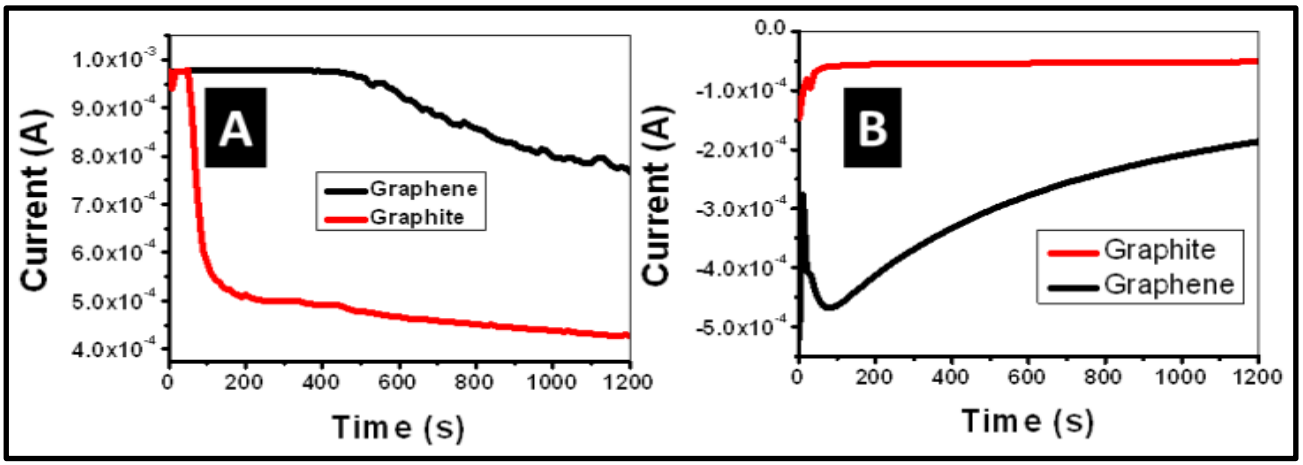


**Fig. 9**. Full flow EFC device performance: (A gives charging behaviour while B gives discharging behaviour)

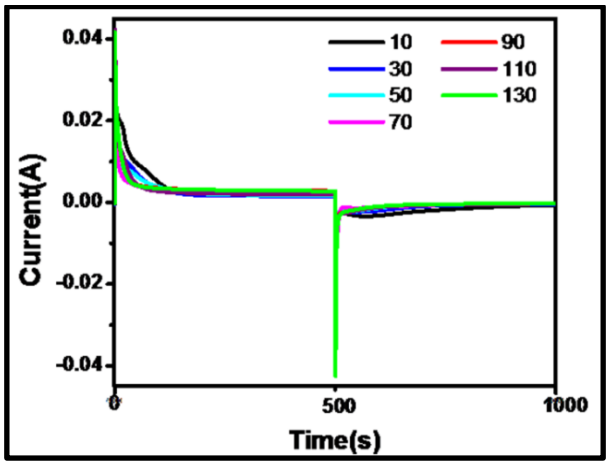


**Fig. 10**. Cycling study of the EFC.

ability to recharge quickly.

## Conclusions

Graphene is a good candidate for use as the carbonaceous material in the slurry of electrochemical flow capacitor. When the layer thickness of graphene reduces, the performance of the system increases. Addition of Faradaic materials into the slurry can improve the energy density. The combination of graphene, isopropyl alcohol, oleyl amine and SLS gives a good composition of storage material for both static and dynamic EDLC based devices. The improved design of EFC can enhance the device performance.

## Acknowledgements

The authors thank the Ministry of New and Renewable Energy (MNRE), Govt. of India for financial support. We acknowledge the technical help from Dr. Sajini Vadukumplly and Ms G. S. Anjusree for TEM and AFM measurements, respectively.

## Notes and references

*Amrita Centre for Nanosciences and Molecular Medicine, Amrita Institute of Medical Sciences, Amrita Vishwa Vidyapeetham, AIMS PO, Ponekkara, Kochi 682041, Kerala, India.*
*E-mail:krvsubramanian@aims.amrita.edu, sreekumarannair@aims.amrita.edu*

† Electronic Supplementary Information (ESI) available: [digital photographs of the spraying equipment and the coated samples, CV and charge - discharge graphs of the comemrcial graphene in ionic electrolyte, Cv studies of graphite electrodes in different electrolytes, a graph showing the flow vs. rpm of the peristaltic pump used]. See DOI: 10.1039/b000000x/

1 (a) N. S. Lewis andD. G. Nocera, *Proc. Natl. Acad. Sci. U. S. A.*, 2006, **43**, 15729-15735. (b) K. G. Reddy,T. G. Deepak, G. S. Anjusree, S. Thomas, S. Vadukumpully, K. R. V. Subramanian, S. V. Nair and A. S. Nair, *Phys. Chem. Chem. Phys*., 2014, **16**, 6838-6858.(c)http://www.iwea.com/index.cfm/page/technologicaldevelopments?twfId=42&download=true.

2 (a) H. Ibrahim, A. Ilinca, and J. Perron, *Renew. Sust. Energ. Rev.*, 2008, **12**, 1221–1250. (b) A. S. Aricò, P. Bruce, B.Scrosati, J.M. Tarascon and W. van Schalkwijk, *Nat. Mater*., 2005, **4**, 366-377.

3 (a) B. Dunn, H. Kamath, and J.-M. Tarascon, *Science*, 2011, **334**, 928-935. (b) P. J. Hall and E. J. Bain, *Energy Policy*, 2008, **36**, 4352-4355.

4 (a) G. Wang, L. Zhang and J. Zhang, *Chem. Soc. Rev*., 2012**, 41**, 797-828, (b) M. Winter and R. J. Brodd, *Chem. Rev*., 2004, **104**, 4245−4269,(c)http://batteryuniversity.com/learn/article/whats_the_role_of_the_supercapacitor.

5 (a) A. Z. Weber, M. M. Mench, J. P. Meyers, P. N. Ross, J. T. Gostick and Q. Liu, *J. Appl. Electrochem*., 2011, **41**, 1137-1164. (b) M. Bartolozzi, *J. Power Sources*, 1989, **27**, 219–234. (c) C. P. de León, A. Frías-Ferrer, J. González-García, D. A. Szánto and F.C. Walsh, *J. Power Sources*, 2006, **160**, 716-732.

6 (a) V. Presser, C. R. Dennison, J. Campos, K. W. Knehr, E. C. Kumbur and Y. Gogotsi, *Adv. Energy Mater*., 2012, **2**, 895–902. (b) V. Presser, C. R. Dennison, J. Campos, K. W. Knehr, E. C. Kumbur and Y. Gogotsi, *Electrochim. Acta*, 2013, **111**, 888 - 897. (c)http://nano.materials.drexel.edu/research/electrochemical-energy-storage/electrochemical-flow-capacitor/

7. V. Presser, C. R. Dennison, J. Campos, K. W. Knehr, E. C. Kumbur and Y. Gogotsi, *Electrochim. Acta*, 2013, **98**, 123-130.

8. (a) Q. Zhang, E. Uchaker, S. L. Candelaria and G. Cao, *Chem. Soc. Rev*., 2013**, 42**, 3127-3171. (b) L. Dai, D. W. Chang, J.-B. Baek and W. Lu, *Small*, 2012, **8**, 1130–1166, (c) M. Pumera, *Energy Environ. Sci*., 2011, **4**, 668-674.

9. (a) C. X. Guo and C. M. Li, *Energy Environ. Sci*., 2011, **4**, 4504-4507. (b) P. Simon and Y. Gogotsi, *Nat. Mater*., 2008, **7**, 845 – 854 (c) Y. Zhai, Y. Dou, D. Zhao, P. F. Fulvio, R. T. Mayes and S. Dai, *Adv. Mater*., 2011, **23**, 4828–4850. (d) Nanotubeshttp://www.natureworldnews.com/articles/6705/20140423ghtweight-cheap-ultracapacitor-built-using-graphene-carbon-nanotubes.htm (e)Fullerenes and Nanotubes: The Building Blocks of Next Generation Nanodevices, Bookedited by Prashant V. Kamat, Dirk M. Guldi, F. DŚouza, Electrochemical Society.

10 R. Aparna, N. Sivakumar, A. Balakrishnan, A. S. Nair, S. V. Nair and K. R. V. Subramanian, *J. Renew. Sustainable Energy*, 2013, **5**, 033123.

11 (a) S. Porada, J. Lee, D. Weingarth and V. Presser, *Electrochem. Commun.*, 2014, DOI: 10.1016/j.elecom.2014.08.023, (b)Theory and Application of Cyclic Voltammetry, fm Measurement of Electrode Reaction Kinetics RICHARD S. NICHOLSON Chemistry Department, Michigan State University, East Lansing, Mich, 11 VOL. 37, NO. 11, OCTOBER 1965 0 1351.

12 http://www.asdlib.org/onlineArticles/elabware/kuwanaEC_lab/PDF-21-Experiment3.pdf

A schematic of an electrochemical flow capacitor device where graphene-based slurries were used as the flow liquids.